Progress in Additive Manufacturing (2023) 8:1489–1499
https://doi.org/10.1007/s40964-023-00415-w

FULL RESEARCH ARTICLE

Laser beam heat treatment in large-scale additive manufacturing

Michel Layher[1] · Lukas Eckhardt[1] · Daniel Linke[1] · Andreas Hopf[1] · Jens Bliedtner[1]

Received: 15 June 2022 / Accepted: 28 January 2023 / Published online: 4 March 2023

Abstract
Large-scale additive manufacturing (LSAM) has been developing a huge potential to address certain tasks in industrial applications over the last years. Particularly granule extrusion technologies enable the processing of an enormous variety of materials but also introduce new challenges in printing large-scale parts. Compared to fused layer modelling and due to larger nozzle diameters as well as higher extrusion rates strand geometry and consequently, process-related voids are enlarged. A promising approach to improve part quality is the integration of carbon dioxide laser (CO_2) radiation into the additive manufacturing process to weld deposited strands by increasing the interface temperature. Experiments are conducted for polymethyl methacrylate (PMMA) and styrene-acrylonitrile (SAN) which are very good absorbers of the wavelength 10.6 µm. Due to the locally defined heat treatment, merely certain areas of the strands are heated to a desired temperature. This leads to a more complete diffusion. At the same time, temperature gradients in the overall part are avoided. By means of a thermographic camera, the temperatures at the re-melting process of deposited strands can be precisely monitored. Therefore, the relation between laser intensity and resulting temperature can be transferred into a repeatable process window. The interaction between laser and deposited material leads to a wider contact area between stacked strands. While flexural strength is not significantly affected, compared to specimens manufactured without any heat treatment bending force is increased by 66% (PMMA) and 48% (SAN), respectively. In addition, voids between adjacent strands are reduced by up to 57%.

Keywords Large-scale additive manufacturing · Material extrusion process · Laser beam heat treatment · Hybrid additive manufacturing · Laser material processing

1 Introduction

The ability to directly transfer three-dimensional models into applicable, additive manufactured parts generates an important requirement to improve research and development as well as design and production processes faster and more efficiently. Among several additive manufacturing (AM) methods, material extrusion processes like fused layer modelling (FLM) have been evolving to one of the most popular technologies for prototyping and small series production.

Since 2016, it is noticed that especially large-scale additive manufacturing (LSAM) systems show a growing availability on the market. Such extrusion systems enhance the variety of materials used for strand deposition and provide high flow rates (> 1.5 kg/h) which lead to a dramatic reduction of manufacturing time [1]. Despite this development, FLM parts provide a multitude of limitations on the utilization in end-use applications, particularly considering their structural and mechanical properties [2]. One of the most dominant issues is the remaining voids between deposited strands [3]. The increase in deposition rates with powerful extrusion systems and larger nozzle diameters (3–15 mm) leads to an upscaling of such process-related part characteristics [4, 5]. This can be found by the manifestation of the staircase effect or the size of cavities appearing on the inside of the components as known from investigations at FLM [6, 7].

Since orthotropic part behaviour is intensified and mechanical properties are strongly dependent on external load orientations, a clear differentiation to injection moulded parts is still necessary. Consequently, LSAM has almost exclusively been used for haptic- or geometric testing and prototyping, respectively. The transformation of orthotropic mesostructures with cavities into (quasi-)isotropic components thus has the potential to bring LSAM prototypes

✉ Michel Layher
michel.layher@eah-jena.de

[1] Ernst-Abbe-University of Applied Sciences Jena, 07745 Jena, Germany

closer to the mechanical properties of injection moulded parts. Such an isotropic performance is especially required at applications with multi-directional loadings and dynamic mechanical environments.

Since parts made by FLM are characterized by orthotropic properties [8–10], the optimization of the interlayer bond has been an important research field within the last years. Important impact on the size of inner structures can be found in void spacing, raster spacing as well as the material flow rate [11, 12]. Other applied methods include process optimization [13–15], material modification [16–18] as well as the integration of devices for additional energy input during the AM process [19–24]. In material extrusion, processes fracture resistance is primarily affected by inter- and intra-layer adhesion as well as void occurrence and size [3, 25]. Current research shows that voids are also minimized when printing temperatures are increased but on the other hand distortion and part deformation might occur as well [2, 3, 15]. In LSAM, this effect is even more present since void size is related to bead dimensions [26]. As distortion also increases with part size, an optimized extrusion temperature is not sufficient to increase part quality of large-scale parts. Instead, additional energy treatments become necessary to re-melt deposited strands and densify the parts. In recent years, several laser heat treatment processes for FLM have been developed, e.g. [19–21, 24, 27, 28]. Based on the FLM principle (Fig. 1), according to DIN EN ISO 17296-2 [29] described by support structure (1), build platform and elevator (2), heated nozzle (3), feedstock supply (4) and product (5), a laser beam system (6) is incorporated as an additional energy source. The laser beam is directed onto deposited beads to reheat defined areas locally. Thus, bonding potential [30, 31] and, consequently, bonding strength can be increased during strand deposition.

Even though there are currently no commercially available machines on the market, various configurations of additive manufacturing systems with additional temperature control are already covered in a large number of patent documents. A variety of approaches incorporate different kinds of laser sources like diode lasers [32–36], solid-state lasers [35, 37–39] as well as infrared lasers [35, 37, 40, 41]. However, the utilization of CO_2 laser radiation for a heat treatment of LSAM parts has not been investigated, yet.

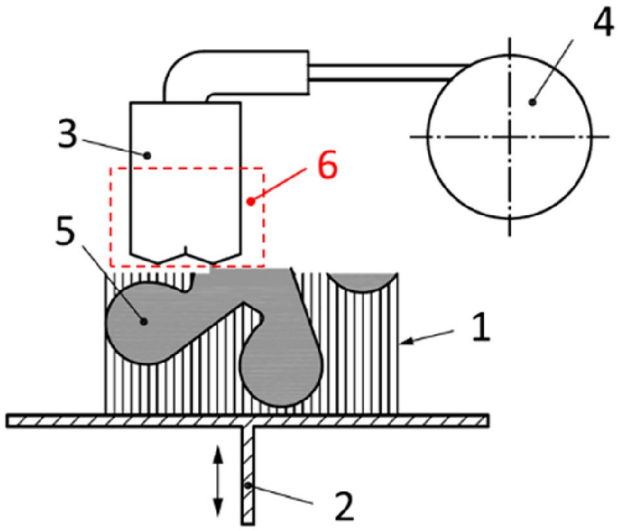

Fig. 1 Enhanced FLM principle according to [29]

2 Setup and methods

The experimental setup utilized for the combined laser extrusion process is commercially not available and has therefore been individually designed. It consists of six main components (Fig. 2). A three-axis linear stage (I), collaboratively developed with Jenaer Antriebstechnik GmbH, realizes maximum build dimensions of 550 mm × 550 mm × 550 mm (x, y, z). The heated build platform (II) provides sufficient

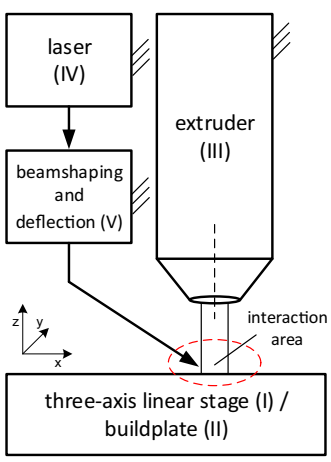

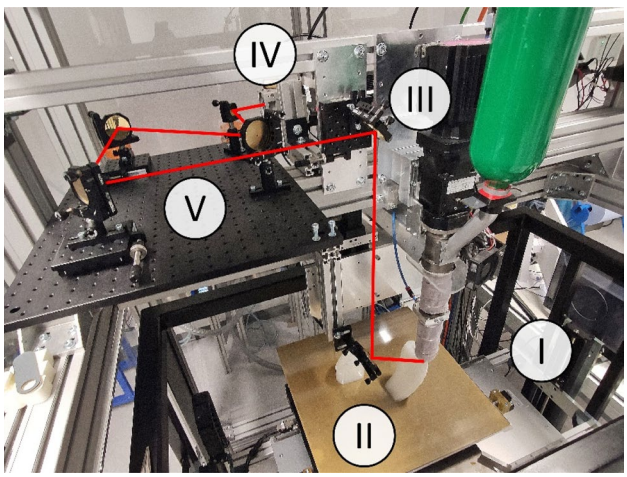

Fig. 2 Enhanced LSAM principle as block diagram (left) and customized experimental setup (right)

adhesion between extruded polymer and printing table. In order to exploit the merits of granule-based extrusion, a single-screw extruder (III), type ExOn10 by Dohle GmbH, is chosen which is equipped with two heater bands and thus two temperatures zones for melting the polymer. It is flexible regarding material selection, and its functionality is unaffected by the vertical mounting. The fixed extruder position enables a continuous deposition process, homogeneous melt flow and repeatable strand geometries, unaffected by kinematic stiffness [42]. The nozzle is a standard configuration of the extruder manufacturer and has an outer diameter of 10 mm and an inner diameter of 3 mm and enables a mass output of up to 6.5 kg/h. Previous investigations on laser beam polished polymers demonstrated that a laser power of $P_{\mathrm{Laser}} = 25$ W is sufficient. Thus, a Synrad 48–2(S) laser system (IV) is integrated. The laser beam travels through a beam shaping unit (V), including a quarter-wave mirror as well as several deflection mirrors. Hence, circular polarized laser radiation and a laser spot of 10.3 mm in diameter are generated within the interaction area on the deposited strand. The overall mechanical design of the manufacturing system allows further extensions like an implementation of the employed infrared camera Optris PI640. It is used for the thermographic measurements during the combined process.

The beam direction is aligned to a fixed position for the entire hybrid manufacturing process. Two different orientations of the laser beam heat treatment are selected for experimental investigations. For modification of the inter layer bond at arrangement A, the laser beam strikes on the deposited material at a vertical angle of $\varphi = 60°$ (Fig. 3, left). The chosen angle serves as a compromise between the dimensions of the mechanical setup and absorption properties of the polymer. At a smaller angle, the beam is impeded by the nozzle which is a result of the given extruder geometry. Larger angles would increase the reflection at the polymer surface [43]. In order to address void reduction, the beam at arrangement B strikes onto the strand at an azimuthal angle of $\psi = 45°$ (Fig. 3, right). Modifications of the optical setup are avoided, since the part orientation on the building platform is changed. Consequently, the laser beam size and the resulting energy distribution are not affected. Under this configuration, the beam spot covers the adjacent strand and extruded strand almost equally.

For the experimental investigations, the materials styrene-acrylonitrile (SAN—TYRIL 790—Trinseo) and polymethyl methacrylate (PMMA—Altuglas VSUVT) are chosen. These unmodified raw materials possess good absorption properties regarding a carbon dioxide (CO_2) laser beam treatment as examined in preceding polishing experiments [44]. The process model for part generation via LSAM is derived according to the findings in previous investigations. Therein, process characteristics regarding bead geometry generation and strand cooling behaviour have been comprehensively examined [45]. This is necessary to guarantee a stable and repeatable manufacturing of specimens.

The settings of the temperature zones for the extruder are highly material and system dependent and therefore iteratively optimized according to [46–48]. Final settings are PMMA: $T_{\mathrm{screw}} = 120$ °C/$T_{\mathrm{nozzle}} = 192$ °C and SAN: $T_{\mathrm{screw}} = 90$ °C/$T_{\mathrm{nozzle}} = 196$ °C. Bead size is defined to $w = 6$ mm (width) and $h = 3$ mm (height). Strand overlap determines the degree to which two adjacent strands occupy the same space within a layer. It is set to its optimum (0.3 mm) in order to gain highest density as well as accurate parts without defects or material adhesion at the nozzle. The laser beam heat treatment is controlled by an independent parameter called irradiation (H) which needs to be introduced for better understanding.

In laser material processing and in accordance with [49], area-related energy is defined by:

$$E = \frac{P_L}{v_s \cdot a_s} \tag{1}$$

E is the area-related energy; v_s is the feed rate of the laser beam; P_L is the laser power; a_s is the line distance.

At arrangement A, the spot size is larger than the bead width. Thus, it becomes necessary to gain the true interaction area between laser beam and polymer by means of a correction value. This is equivalent to the percentage of the laser power within the limits of the bead width and can be obtained using the intensity profile of the Gaussian beam. A correction value of 75.6% is derived for the setup, and the adapted formulation for the irradiation is gained by:

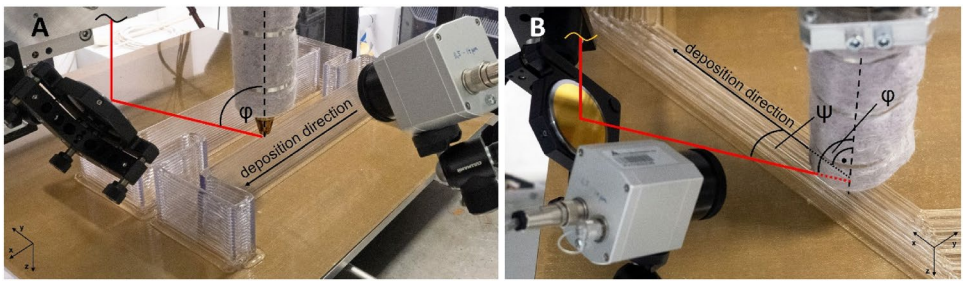

Fig. 3 Orientations for laser beam heat treatment—arrangement **A** (left) and arrangement **B** (right)

$$H = \frac{P_L \cdot 0,756}{v_f \cdot w} \tag{2}$$

H is the irradiation; v_f is the feed rate of the print platform P_L is the laser power; w is the bead width

Due to a defined bead width, feed rate is at a constant value and, consequently, the process is directly controllable by the applied laser power. Laser beam heat treatment only is conducted along negative x-direction.

Samples for flexural testing are gained from parts manufactured at approach A. The flexural strength is obtained via 4-point flexural test according to DIN EN ISO 14125 [50]:

$$\sigma_f = \frac{F \cdot L}{b_p \cdot {h_p}^2} \tag{3}$$

σ_f is the flexural strength; h_p is the thickness of the specimen (DIN); F is the force (measured); b_p is the width of the specimen (DIN); L is the supporting width (const.)

Specimens made of large-scale single strands realize the standardized testing geometry only in approximation. Thus, it is necessary to correct the measured values under consideration of the real contact length (K) of adhered strands. This condition is explained in a simplified illustration (Fig. 4).

In this case, the specimen's width (b_p) is defined by previous sawing which leads to deviations of up to ± 0.2 mm. The process setting for bead width (w) describes the specimen's thickness according to DIN (h_p). When the flexural test is conducted, a force (F) is determined relating to the real, reduced contact length (K). Consequently, the corrected flexural strength is gained by:

$$\sigma' = \frac{F \cdot L}{b_p \cdot K^2} \tag{4}$$

σ' is the flexural strength; K is the real contact length (measured); F is the force (measured); b_p is the width of the specimen (measured); L is the supporting width (const.)

Hence, an underestimation of the flexural strength is avoided. In addition, this condition is essential to delineate the effect of contact zone increment due to laser beam heat treatment quantitatively. Samples of approach B (cross sections) are examined via microscope. A software allows to detect the ratio between solid material and existing voids.

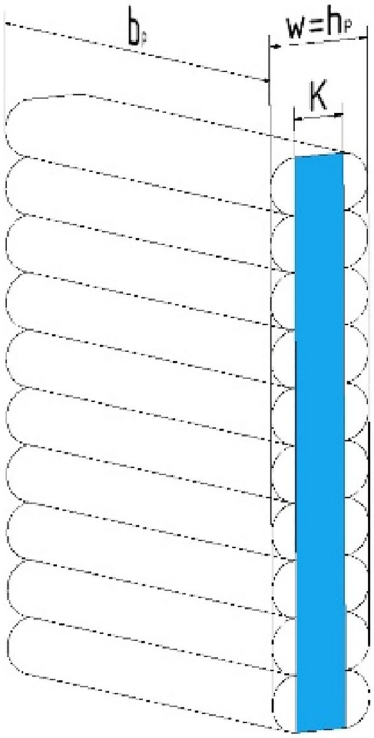

Fig. 4 Illustration of the real contact length (K)

3 Results and discussion

3.1 Vertical bonding of layered single strands

Investigations of the hybrid manufacturing process regarding the vertical bonding are conducted for hollow cuboids and in accordance with arrangement A (cf. Fig. 3, left). During the deposition of layered polymer strands, laser energy is induced into the material.

Results display a linear relationship between irradiation (cf. formula (2)) and temperature rise (ΔT) within the interaction area (Fig. 5).

Thus, it is ensured that process control is given by an alteration of laser power and the irradiation $H_{PMMA} \leq 150$ mJ/mm^2 and $H_{SAN} \leq 140$ mJ/mm^2, respectively. If the respective irradiation values are exceeded, degradation processes of the plastic occur due to the excessive heat accumulation. The decomposition temperatures known from the literature are $T_{dec/PMMA} = 280$ °C [51] and SAN $T_{dec/SAN} = 250$ °C [52]. Reaching these temperatures leads to the formation of smoke. The determination of the maximum spot temperature by means of a thermographic measurement also confirms the theoretical values, although such an absolute measurement is only valid as an approximation. The significantly larger standard deviations around the gained temperature mean values at $H_{PMMA} > 150$ mJ/mm^2 and $H_{SAN} > 140$ mJ/mm^2 are a further indicator of changes in the polymers' structure and the beginning of decomposition. The limit for irradiation is therefore essential for the process control of laser beam heat treatment. Decomposition processes are also known from studies on laser beam heat treatment of FLM parts [19, 27, 28] and, moreover, in agreement with the characteristic curve of laser beam welding of polymers [52, 53].

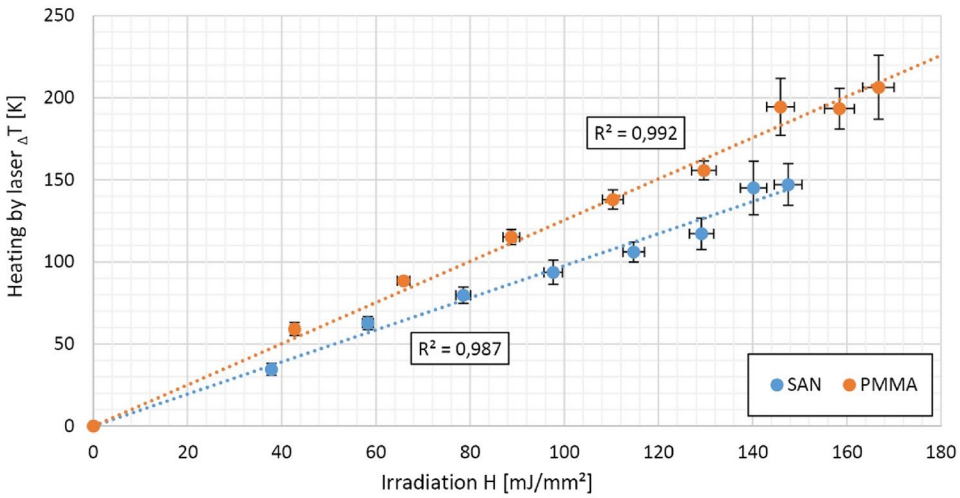

Fig. 5 Coherence between irradiation and temperature increase in the material within the interaction area for PMMA and SAN

After the manufacturing, specimens are cut out with the dimension $h_p \times b_p = 6$ mm × 15 mm and a 4-point flexural test is conducted according to DIN EN ISO 14125 [50]. The fracture zones are investigated in order to gain the values of $K \times b_p$ (cf. Fig. 4). Under consideration of the real contact area, the evaluation of the flexural strength reveals laser beam heat treatment has no improvement regarding the quality of the material bond between the layers (Fig. 6). The average values $\sigma_{PMMA} = 26.2 \pm 2.5$ MPa and $\sigma_{SAN} = 41.8 \pm 4.2$ MPa are determined.

Since there is no increase in flexural strength, it is concluded that in LSAM diffusion processes between two consecutive strands are not improved by a laser beam treatment. Thus, deposited strands possess not only enough energy for diffusion and randomization mechanisms [45] but also bonding mechanisms appear to be unaffected by the combined process. However, strand temperature will decrease over time, especially when extrusion paths are very long, e.g. for big part sizes. This increase in process time eventually leads to a significant temperature difference between the deposited polymer strand and the layer underneath. Under these conditions, it is expected that the effect of a laser beam heat treatment becomes noticeable. Also, industrial applications tend to increase the printing speed of their processes. This requires, for example, cooling fans to lock the deposited material in shape. Laser heating could enhance such applications and enable faster printing without compromising print speed or bond strength. However, since there are contrary findings regarding the effects of dispensed air on deposited strands [31, 54, 55], this approach needs to be further examined for LSAM processes.

Furthermore, the experimental results show that the formation of the contact length K, especially above a value of $H > 100$ mJ/mm^2, is strongly influenced by the irradiation. Hence, in approximation a linear trend can be derived for both parameters (Fig. 7).

The additional energy input leads to an increase in molecular motion as well as a local strand softening. When

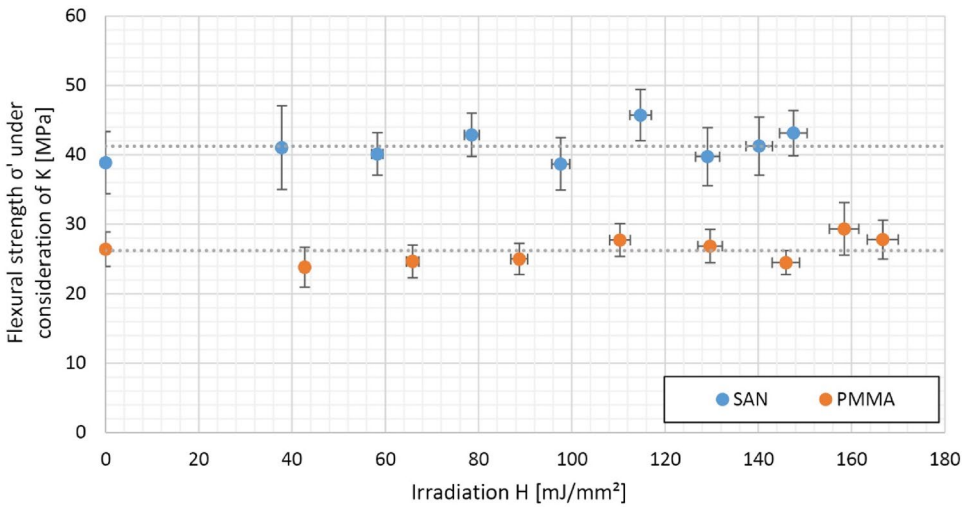

Fig. 6 Irradiation-dependent flexural strength for PMMA and SAN

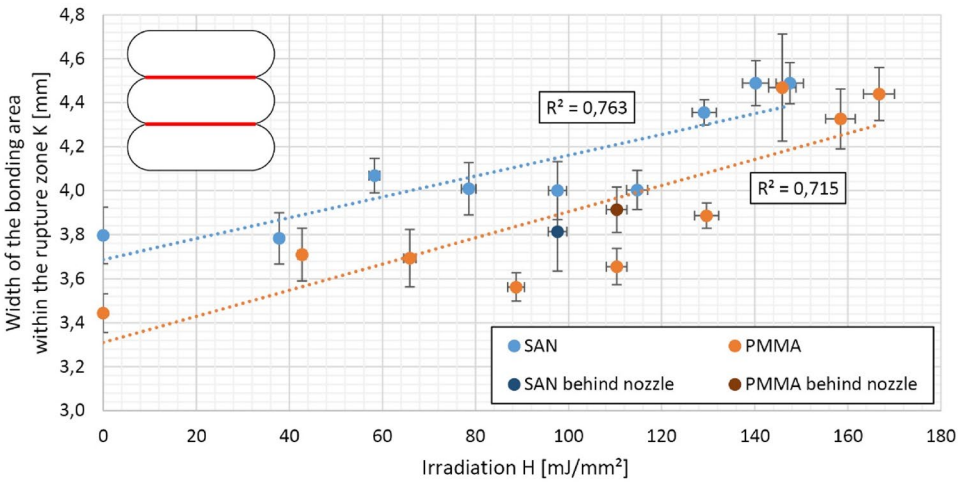

Fig. 7 Irradiation impact on the contact length (*K*)

the material is deposited, a compressive force acts on the strand underneath. This results in displacement of the material melted by laser radiation at the strand surface. Contact length K increases by 26% for PMMA and by 13% for SAN. The measurement points on PMMA, deviating from the trend line, are particularly striking. The reason can be found in the strong variation of the strand width. This effect is caused by the used extrusion system and particularly noticeable when PMMA is processed. Nevertheless, a correlation between laser beam energy input and the resulting change in the interlayer bonding surface can be derived.

The gained results show that laser beam heat treatment leads to a broadening of the interlayer connection and, consequently, to an increase in the contact length K (cf. Fig. 7). At the same time, no increase in the corrected flexural strength σ' can be found (cf. Fig. 6). This leads to the conclusion that σ' remains unaffected by laser energy input. However, due to the uniform specimen geometry, there is a constant relationship between the quantities F and K (cf. formula (4)). Since K is enlarged due to the laser energy input, the bending force required for component fracture increases as well (Fig. 8).

Therefore, the result is not to be interpreted as an improvement in the material bond but rather as an improvement in the geometric layer quality and, thus, a higher resistance behaviour under load. The increase in K represents a mechanical change in the component structure, which contributes to the increase in component strength independently of the material properties. Compared to previously conducted investigations at standard LSAM components, the bending force is increased by 66% for PMMA and 48% for SAN.

This result is also favoured by the changed surface profile of the components (Fig. 9). The increase in K significantly reduces the for LSAM typical notch formation between two vertically bonded, consecutive strands. Besides the enlarged interlayer connection notch effect is reduced, which has a positive effect on the absorption of external forces [56, 57].

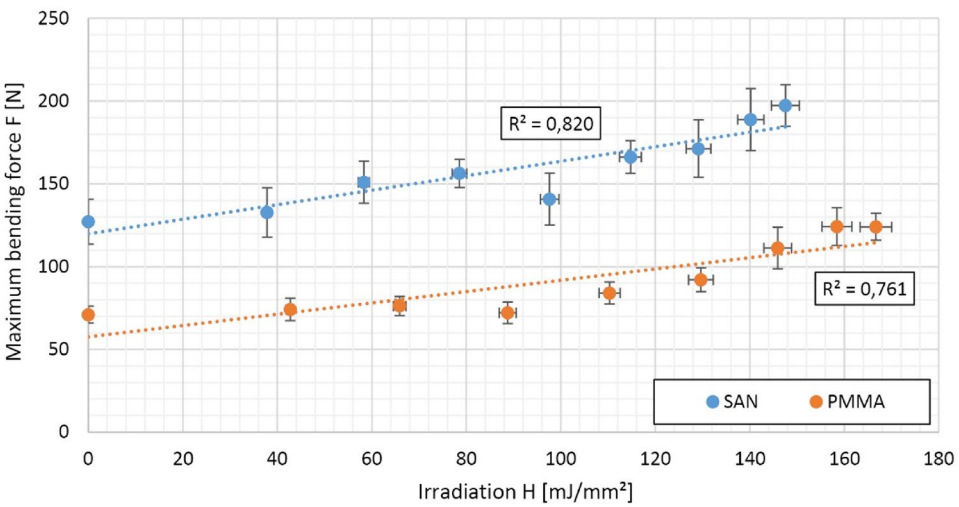

Fig. 8 Irradiation impact on the bending force

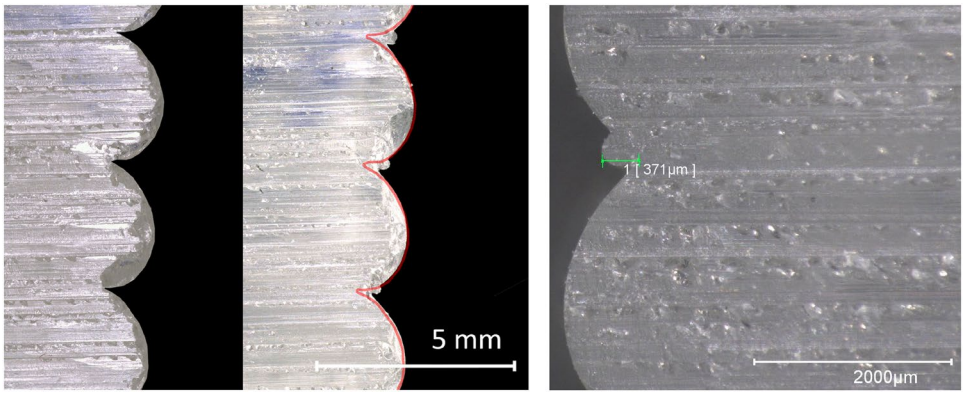

Fig. 9 For PMMA, contact length and notch formation after extrusion and overlay of broadening of K and notches as well as notch reduction due to laser beam heat treatment in detail (right)

The modified interlayer connection is clearly more dominant for PMMA than for SAN. For both materials and despite the increase in contact length and the associated smoothing of the notch (cf. Fig. 9 right), no influence on the overall component height (along the z-orientation) is discernible. Furthermore, it can be noticed that the maximum temperatures, which occur at high irradiation, are already in the decomposition range of the polymers but appear to have no influence on the component properties within the conducted investigations.

3.2 Lateral laser beam treatment and void reduction

Investigations of the hybrid manufacturing process regarding the lateral laser beam treatment are conducted for multiple-strand parts and in accordance with arrangement B (cf. Fig. 3, right). In doing so, it is investigated whether process-characteristic voids can be reduced.

Due to the oblique incidence of the laser radiation on the strand surface, it is not possible to clearly determine the actual value of the irradiation in this configuration. Therefore, for the examination, the laser power is set to $P_{\text{Laser-SAN}} = 22$ W and $P_{\text{Laser-PMMA}} = 19$ W based on preliminary tests. In addition, a strand overlap of 0.3 mm is applied (Fig. 10).

Considering the cross-sectional view, the laterally irradiated part (Fig. 11, right) and the corresponding non-irradiated reference part (Fig. 11, left) show clear differences regarding void size. Due to the laser energy input, these process-typical features are significantly less dominant for both PMMA and SAN. At the same time, no change in the shape of the component is discernible. Thus, the hybrid process actively contributes to the transition from orthotropic- to (quasi)isotropic component properties without impairing the dimensional shape of the component produced.

Due to the underlying process windows for the strand deposition and the tempering process, the possibilities for a further process optimization are severely limited. Merely the parameter strand overlap remains as a variable which can be varied independently of the strand model and at the same time, within certain limits, does not influence the effect of the hybrid process. For this reason, the strand overlap is iteratively increased in a subsequent step under constant process conditions.

Since lateral melting of deposited strands is associated with a local viscosity reduction, a higher overlap between two adjacent strands is enabled. The extruded strand forces the liquified material towards the void leading to a denser

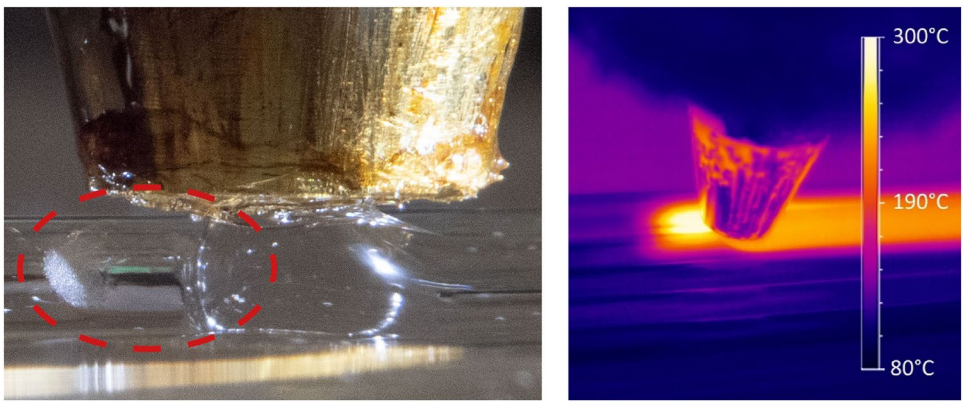

Fig. 10 Lateral laser beam heat treatment for PMMA with highlighted interaction area (left) and thermographic measurement (right)

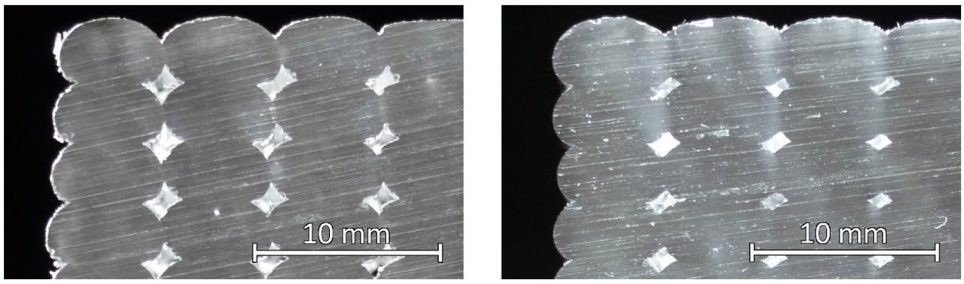

Fig. 11 Cross-sectional view of specimens made by LSAM (left) and the hybrid process (right) depicted for PMMA

part structure. Experiments show that the maximum overlap for PMMA and SAN can be increased from 0.3 to 0.5 mm.

In a direct comparison between the extrusion and hybrid process, for LSAM a distortion of the component structure occurs, which is particularly evident from the shifted void formation (cf. Fig. 12, left). Strand viscosity is too high, and therefore, adjacent strands are rather stacked diagonally than bonded laterally for an overlap of 0.5 mm. This leads to an alteration of the deposited bead geometry and eventually to a distortion of the part structure. As a consequence, void size is reduced due to overfilling. This effect is intensified along the manufacturing direction (from the left to the right) and will become even more visible at the surfaces of larger parts. In the hybrid process, lateral offset is not present and strand shape is retained (cf. Fig. 12, right). Again, voids appear to be more reduced at the right-hand side of the sectional view. The manufacturing from the left to the right results in a superimposition of lowered strand viscosity due to heat accumulation, additional energy input by the laser beam heat treatment and higher overlap. Hence, void size diminution is also tool-path dependent.

However, for the investigated specimen size, laser LSAM does not lead to distortions. Utilizing the Keyence VHX-7000 measuring microscope, the void areas can be detected and compared to each other. In doing so, the number of pixels within a defined measuring field (red box) is counted. Voids can clearly be separated due to the difference in colour. This enables a sharp distinction of polymer structure and void formation. Thus, the pixels of the void areas are gained as percentage of the entire measuring field. It is found that the laser energy deposition achieves a void reduction of up to 28% for PMMA and 57% for SAN.

The delineated experiments on laser beam heat treatment in LSAM illustrate the huge potential of the hybrid process. In particular, the reduction of process-characteristic voids in the area of intra-laminar strand bond leads to a significant improvement in LSAM part density. Lateral laser treatment makes it possible to overcome limiting conditions of strand deposition with regard to overlap. The filling level of large-volume components is significantly optimized, while part shape is maintained. This also allows a further transition from an orthotropic to a (quasi)isotropic component structure.

4 Summary and outlook

An experimental setup for large-scale additive manufacturing (LSAM) is enhanced by a CO_2-laser system and several beam deflection units in order to realize a hybrid manufacturing process. For laser beam heat treatment, two different ways of orientations are chosen. Experiments are conducted with PMMA (Altuglas VSUVT) and SAN (TYRIL 790—Trinseo).

Initially, vertical bonding of layered single strands is investigated for hollow cuboids. A linear relationship between irradiation (H) and temperature rise (ΔT) within the interaction area is gained. Process control is given by an

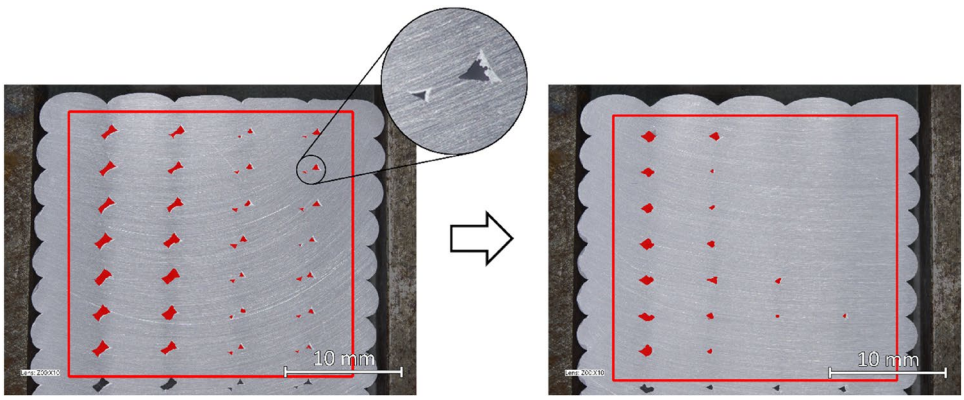

Fig. 12 Cross-sectional view of the achieved void reduction (highlighted) for LSAM (left) and hybrid LSAM (right)—depicted for SAN with an overlap of 0.5 mm

alteration of laser power and the irradiation $H_{PMMA} \leq 150$ mJ/mm^2 and $H_{SAN} \leq 140$ mJ/mm^2, respectively. As respective irradiation values are exceeded, degradation processes of the plastic occur.

Additionally, a 4-point flexural test is conducted according to DIN EN ISO 14125 [50]. It reveals that under consideration of the real contact area between two strands, laser beam heat treatment shows no improvement regarding the quality of the material bond between the layers. Average values of $\sigma_{PMMA} = 26.2 \pm 2.5$ MPa and $\sigma_{SAN} = 41.8 \pm 4.2$ MPa are determined.

Furthermore, results show that laser beam heat treatment influences contact length (K) between two vertical bonded strands, especially at $H > 100$ mJ/mm^2. In approximation, a linear trend between K and H can be derived. Contact length K increases by 26% for PMMA and by 13% for SAN.

However, corrected flexural strength (σ') remains unaffected by laser energy input, but bending force, required for component fracture, is increased. The enlarged K represents a mechanical change in the component structure, which contributes to the increase in component strength independently of the material properties. Compared to a standard LSAM component, the bending force is increased by 66% for PMMA and 48% for SAN. Also, for LSAM typical notch formation between two vertically bonded strands is mitigated, which has a positive effect on the absorption of external forces [56, 57]. This modified interlayer connection is more dominant for PMMA than for SAN, and no influence on the overall component height (along the *z*-orientation) is discernible.

Lateral laser beam treatment clearly leads to a void reduction. At the same time, no change in the shape of the manufactured component is discernible. Thus, the hybrid process actively contributes to the transition from orthotropic- to (quasi)isotropic component properties without impairing the dimensional shape of the component produced. Furthermore, the maximum overlap for PMMA and SAN can be increased from 0.3 to 0.5 mm due to the laser energy input. A void reduction by approximately 28% for PMMA and 57% for SAN is achieved.

In summary, laser beam heat treatment in large-scale additive manufacturing has a huge potential not only to reduce process-characteristic voids in the area of intralaminar strand bond but also to significantly improve part density and inter-strand contact length.

Since the delineated results are mainly limited due to the mechanical setup, which only achieves a unidirectional hybrid process, further improvements become necessary. Particularly, for standardized extrusion processes, the laser beam needs to be guided along the path of extrusion to cover the entire component. Therefore, the experimental setup will be enhanced by a laser beam deflection system according to [58]. So, it becomes possible to investigate the hybrid process close to industrial conditions [59] and for a wider range of materials.

Funding Open Access funding enabled and organized by Projekt DEAL. Funding was provided by Bundesministerium für Wirtschaft und Klimaschutz (BMWK), KK5091602SK0.

Data availability The data supporting the findings of this study are available within the article.

References

1. Justino Netto JM, Idogava HT, Frezzatto Santos LE, Silveira ZdC, Romio P, Alves JL (2021) Screw-assisted 3D printing with granulated materials: a systematic review. In: The International Journal of Advanced Manufacturing Technology, 1–17
2. Turner BN, Gold SA (2015) A review of melt extrusion additive manufacturing processes: II. Materials, dimensional accuracy, and surface roughness. Rapid Prototyp J 21(3):250–261
3. Aliheidari N, Christ J, Tripuraneni R, Nadimpalli S, Ameli A (2018) Interlayer adhesion and fracture resistance of polymers printed through melt extrusion additive manufacturing process. Mater Des 156:351–361
4. Duty CE, Kunc V, Compton B, Post B, Erdman D, Smith R, Lind R, Lloyd P, Love L (2017) Structure and mechanical behavior of Big Area Additive Manufacturing (BAAM) materials. Rapid Prototyp J 23(1):181–189
5. Shah J, Snider B, Clarke T, Kozutsky S, Lacki M, Hosseini A (2019) Large-scale 3D printers for additive manufacturing: design considerations and challenges. Int J Adv Manuf Technol 104(9–12):3679–3693
6. Anitha R, Arunachalam S, Radhakrishnan P (2001) Critical parameters influencing the quality of prototypes in fused deposition modelling. J Mater Process Technol 118(1–3):385–388
7. Bakar NSA, Alkahari MR, Boejang H (2010) Analysis on fused deposition modelling performance. J Zhejiang Univ SCIENCE A 11(12):972–977
8. Casavola C, Cazzato A, Moramarco V, Pappalettere C (2016) Orthotropic mechanical properties of fused deposition modelling parts described by classical laminate theory. Mater Des 90:453–458
9. Domingo-Espin M, Puigoriol-Forcada JM, Garcia-Granada A-A, Llum J, Borros S, Reyes G (2015) Mechanical property characterization and simulation of fused deposition modeling Polycarbonate parts. Mater Des 83:670–677
10. Lohr W, Härtel A, Reinicke T (2018) Ermittlung von Materialkennwerten für additiv gefertigte Bauteile im Kreuzverbund nach dem FDM-Verfahren zur numerischen Berechnung der Festigkeitseigenschaften

11. Gao X, Qi S, Kuang X, Su Y, Li J, Wang D (2021) Fused filament fabrication of polymer materials: a review of interlayer bond. Addit Manuf 37:101658
12. Goh GD, Yap YL, Tan HKJ, Sing SL, Goh GL, Yeong WY (2020) Process–structure–properties in polymer additive manufacturing via material extrusion: a review. Crit Rev Solid State Mater Sci 45(2):113–133
13. Ahn S-H, Montero M, Odell D, Roundy S, Wright PK (2002) Anisotropic material properties of fused deposition modeling ABS. Rapid Prototyp J 8(4):248–257
14. Abbott AC, Tandon GP, Bradford RL, Koerner H, Baur JW (2018) Process-structure-property effects on ABS bond strength in fused filament fabrication. Addit Manuf 19:29–38
15. Kuznetsov VE, Solonin AN, Tavitov AG, Urzhumtsev OD, Vakulik AH (2018) Increasing of strength of FDM (FFF) 3D printed parts by influencing on temperature-related parameters of the process
16. Levenhagen NP, Dadmun MD (2018) Interlayer diffusion of surface segregating additives to improve the isotropy of fused deposition modeling products. Polymer 152:35–41
17. Shaffer S, Yang K, Vargas J, Di Prima MA, Voit W (2014) On reducing anisotropy in 3D printed polymers via ionizing radiation. Polymer 55(23):5969–5979
18. Wang Z, Liu R, Sparks T, Liou F (2016) Large-scale deposition system by an industrial robot (I) design of fused pellet modeling system and extrusion process analysis. 3D Print Addit Manuf, 3(1):39–47
19. Han P, Tofangchi A, Deshpande A, Zhang S, Hsu K (2019) An approach to improve interface healing in FFF-3D printed Ultem 1010 using laser pre-deposition heating. Procedia Manuf 34:672–677
20. Luo M, Tian X, Zhu W, Li D (2018) Controllable interlayer shear strength and crystallinity of PEEK components by laser-assisted material extrusion. J Mater Res 33(11):1632–1641
21. Luo M, Tian X, Shang J, Zhu W, Li D, Qin Y (2019) Impregnation and interlayer bonding behaviours of 3D-printed continuous carbon-fiber-reinforced poly-ether-ether-ketone composites. Compos A Appl Sci Manuf 121:130–138
22. Kishore V, Ajinjeru C, Nycz A, Post B, Lindahl J, Kunc V, Duty C (2017) Infrared preheating to improve interlayer strength of big area additive manufacturing (BAAM) components. Addit Manuf 14:7–12
23. Shih C-C, Burnette M, Staack D, Wang J, Tai BL (2019) Effects of cold plasma treatment on interlayer bonding strength in FFF process. Addit Manuf 25:104–111
24. Kühn C, Niese B, Witt G (2019) Verbesserung der mechanischen Eigenschaften im FLM-Verfahren durch lokale Laservorerwärmung und Endlosfaserverstärkung. In: Proceedings of the 16th Rapid.Tech Conference Erfurt, Germany, 25–27 June 2019, 258–273
25. Papon EA, Haque A, Mulani SB (2019) Process optimization and stochastic modeling of void contents and mechanical properties in additively manufactured composites. Compos B Eng 177:107325
26. Eiliat H, Urbanic J (2018) Visualizing, analyzing, and managing voids in the material extrusion process. Int J Adv Manuf Technol 96(9–12):4095–4109
27. Ravi AK, Deshpande A, Hsu KH (2016) An in-process laser localized pre-deposition heating approach to inter-layer bond strengthening in extrusion based polymer additive manufacturing. J Manuf Process 24:179–185
28. Deshpande A, Ravi A, Kusel S, Churchwell R, Hsu K (2019) Interlayer thermal history modification for interface strength in fused filament fabricated parts. Prog Addit Manuf 4(1):63–70
29. [DIN EN ISO 17296–2] Additive Fertigung - Grundlagen - Teil 2: Überblick über Prozesskategorien und Ausgangswerkstoffe. DEUTSCHE NORM; Dezember 2016. DIN Deutsches Institut für Normung e.V., Berlin, Ref. Nr. 17296–2:2016, Beuth Verlag GmbH, 10772 Berlin.
30. Yardimci MA, Güçeri S (1996) Conceptual framework for the thermal process modelling of fused deposition. Rapid Prototyp J 2(2):26–31
31. Yan Y, Zhang R, Hong G, Yuan X (2000) Research on the bonding of material paths in melted extrusion modeling. Mater Des 21(2):93–99
32. Hsu K (2016) Systems and Methods for Laser Preheating in Connection with fused deposition modeling Patent US 10710353 B2
33. Parthy K (2016) Verzugs-Reduzierung von Kunststoffteilen, Apparatur und Verfahren, insbesondere von im 3D-Druck erstellten Teilen. FDM-Drucker DE 102015007349:A1
34. Gordon M (2015) Increased inter-layer bonding in 3D printing Patent US 9339972 B2
35. Nixon JR, Newell Cu, Diekmann T (2019) Laser Preheating in Three-Dimensional Printing US 2020055239 A1
36. Hsu K (2016) Systems and Methods for Laser Preheating in Connection with fused deposition modeling US 20170072633 A1
37. Mok SSC, Chong YH, Bong TKu, Toh DJ (2002) A method and apparatus for producing a prototype WO 02073325 A2
38. McGregor G, Islam M-U, Xue Lu Campbell G (2000) Laser consolidation methodology and apparatus for manufacturing precise structures Patent US 6504127 B1
39. Islam M-U, Xue Lu, McGregor G (1999) Process for manufacturing or repairing turbine engine or compressor components Patent CA 2284759 C
40. Tierney Ju, King T (2017) Temperature regulation to improve additive 3D printing function Patent US 11034142 B2
41. Wei Z, Du J, Lu Bu, Wang J (2014) Front heating and monitoring device of laser beam for 3D printing Patent CN 103895227 A
42. Schoeppner V, Schumacher C, Guntermann J (2017) Beurteilung der Schweißnahtfestigkeiten verschiedener Kunststoffe im FDM-Prozess. Jahresmagazin Kunststofftechnik, 108–114
43. Poprawe R (2011) Tailored Light 2. Berlin, Heidelberg: Springer Berlin Heidelberg
44. Layher M, Hopf A, Eckhardt L, Bliedtner J (2019) Laser beam polishing of polymers. Photon Views 16(3):83–87
45. Layher M, Eckhardt L, Hopf A, Bliedtner J (2021) Development of a process model for bead deposition rates and cooling behavior of large scale additive manufacturing parts. In: Industrializing Additive Manufacturing – AMPA, 223–240
46. Campbell GAu, Spalding MA (2013) Analyzing and troubleshooting single-screw extruders. München: Hanser. https://doi.org/10.3139/9783446432666
47. Del Pilar Noriega EM, Rauwendaal C (2019) Troubleshooting the extrusion process. A systematic approach to solving plastic extrusion problems. Hanser eLibrary. München: Hanser
48. Limper A (2013) Verfahrenstechnik der Thermoplastextrusion. Hanser, München
49. Bliedtner J, Müller H, Barz A (2013) Lasermaterialbearbeitung. Grundlagen - Verfahren - Anwendungen - Beispiele. München: Carl Hanser Fachbuchverlag. http://www.hanser-elibrary.com/action/showBook?doi=10.3139/9783446429291
50. [DIN EN ISO 14125:2011-05] Faserverstärkte Kunststoffe - Bestimmung der Biegeeigenschaften. DEUTSCHE NORM; Mai 2011. DIN Deutsches Institut für Normung e.V., Berlin, Ref. Nr. 14125:2011-05, Beuth Verlag GmbH, 10772 Berlin.
51. Ehrenstein G (2011) Polymer-Werkstoffe. Struktur; Eigenschaften; Anwendung. s.l.: Carl Hanser Fachbuchverlag
52. Gillner A (2009) Laser in der Kunststofftechnik. Heidelberg, München, Landsberg, Frechen, Hamburg: Hüthig
53. Russek UA, Palmen A, Staub H, Poehler J, Wenzlau C, Otto G, Poggel M, Koeppe A, Kind H (2003) Laser beam welding of thermoplastics, 458

54. Prajapati H, Salvi SS, Ravoori D, Qasaimeh M, Adnan A, Jain A (2021) Improved print quality in fused filament fabrication through localized dispensing of hot air around the deposited filament. Addit Manuf 40:101917
55. Partain SC (2007) Fused deposition modeling with localized pre-deposition heating using forced air. Master Thesis. Bozeman, Montana. https://scholarworks.montana.edu/xmlui/handle/1/2016
56. Grellmann W, Seidler S (2015) Kunststoffprüfung. München: Carl Hanser Verlag. https://doi.org/10.3139/9783446443907
57. Frick A, Stern C (2011) Praktische Kunststoffprüfung. München: Hanser
58. Layher M, Bliedtner J, Theska R (2021) Development of a laser beam deflection system for hybrid large scale additive manufacturing. euspen's 21st International Conference & Exhibition, Copenhagen, DK, June 2021. In: Proceedings of the 21st International Conference of the European Society for Precision Engineering and Nanotechnology, 75–78
59. Layher M, Bliedtner J, Theska R (2022) Hybrid additive manufacturing. Photon Views 19(5):47–51